行政院國家科學委員會專題研究計畫成果報告

釔氧2116系相圖，鎢氧化物磁性與導電性質，及123銅氧系的自旋能隙與Tc壓抑現象之研究

計畫類別：☑個別型計畫　□整合型計畫

計畫編號：NSC88—2112--M032-008

執行期間：87年8月1日至88年7月31日

個別型計畫：計畫主持人：錢凡之
共同主持人：

整合型計畫：總計畫主持人：
子計畫主持人：

註：整合型計畫總報告與子計畫成果報告請分開編印各成一冊，彙整一起繳送國科會。

處理方式：□可立即對外提供參考
（請打ｖ）☑一年後可對外提供參考
□兩年後可對外提供參考
（必要時，本會得展延發表時限）

執行單位：淡江大學物理系

中華民國　89年2月25日

Journal of Superconductivity, Vol. 11, No. 6, 1998

Spin Gap Effects on Bulk $R_{1+x}Ba_{2-x}Cu_3O_{7-\delta}$ (R = Eu or Nd and $0 \le x \le 0.4$)

Cheng Yi You,[1] Fan Z. Chien,[1] and Weiyan Guan[2]

Spin gap effects on the underdoping states of the bulk system of $R_{1+x}Ba_{2-x}Cu_3O_{7-\delta}$ (R = Eu or Nd and $0 \le x \le 0.4$) were investigated through transport property measurements. The underdoping states were achieved by, alternatively substituting R^{3+} for Ba^{2+} ions in the system rather than adjusting the oxygen deficiency. The excess R^{3+} ions were to occupy the Ba sites of the crystalline lattice as revealed from Rietveld analysis for powder X-ray diffraction. The underdoped materials were observed to first undergo spin pairing transition in the temperature range well above T_c, and come across with superconducting transition at T_c. The increasing feature observed for spin gap temperature and the decreasing one for T_c, as the concentration of holes decreases, are in qualitatively good agreement with theoretical predictions from the mean-field RVB model.

KEY WORDS: High-T_c superconductors; spin gap; electronic transport.

1. INTRODUCTION

The resonant-valence-bond (RVB) model, where spin and charge degrees of freedom are separated, was proposed in 1987 by P. W. Anderson [1] to account for the newly discovered high-T_c superconductivity [2,3]. Based on the RVB model, Nagaosa and Lee [4] had worked out detailed calculations and drawn a mean-field phase diagram for various hole-dopant states of the high-T_c superconductors. They concluded that there exist an intermediate state, the spin gap, between the states of the high-T_c superconductor and the strange metal, in which linear relations between resistivity and temperature were observed throughout the temperature range above T_c. And the spin gap temperature (T_s) is expected to increase as the concentration of holes decreases, and vice versa for T_c. Similar conclusions were drawn from the analysis of the low-temperature London penetration depth by Emery and Kivelson [5].

Experimentally, Warren *et al.* [6] suggested the possible onset of spin pairing in individual planes of oxygen-deficient $YBa_2Cu_3O_{6+x}$ well above the superconducting transition temperature for three-dimensional bulk through nulcear spin-lattice relaxation measurements. As revealed from subsequent investigations in nuclear quadruple resonance and nuclear magnetic resonance measurements on $Y(Ba_{1-x}La_x)Cu_3O_7$ [7] and underdoped $YBa_2Cu_3O_{6+x}$ [8], respectively, the spin-lattice relaxation rate per unit temperature $(T_1T)^{-1}$ measured at planar ^{17}O sites decreases with temperature and that at ^{63}Cu sites peaks at T_s. While in optimally doped $YBa_2Cu_3O_{6+x}$ [6], $(T_1T)^{-1}$ at ^{63}Cu sites has a monotonous temperature dependence and that at planar ^{17}O sites is essentially temperature independent above T_c. In view of the evidence, the opening of the pseudogap in the spin excitation spectrum was suggested. And it was in turn confirmed through the neutron-inelastic scattering experiments on oxygen-deficient $YBa_2Cu_3O_{6+x}$ [9,10].

The most profound evidence is the observation of the pseudogap in the normal state of underdoped $Bi_2Sr_2CaCu_2O_{8+y}$ [11,12] using the angle-resolved photoemission spectroscopy in which the momentum-resolved electron excitation spectrum of the

[1]Department of Physics, Tamkang University, Tamsui, Taiwan, Republic of China.
[2]Department of Physics, National Tsing Hua University, Hsinchu, Taiwan, Republic of China.

0896-1107/98/1200-0693$15.00/0

CuO_2 planes were directly measured. As a result, the close relation between the normal-state pseudogap above T_c and the superconducting gap below T_c was suggested.

The in-plane resistivity for the underdoped $YBa_2Cu_3O_{6+x}$ [13,14], in the temperature range well above T_c, was found to start deviating appreciably from the T-linear behavior, which is expected in the normal state of an optimally doped RBCO, at T_s. Similar conclusions were made through investigations in $YBa_2Cu_4O_8$ [15].

In this report, spin gap effects on the underdoping states of the bulk system of $R_{1+x}Ba_{2-x}Cu_3O_{7-\delta}$, where R = Eu or Nd and $0 \le x \le 0.4$, were investigated through transport property measurements. The underdoping states were achieved by alternatively substituting R^{3+} for Ba^{2+} ions in the system rather than adjusting the oxygen deficiency. The excess R^{3+} ions were to occupy the Ba sites of the crystalline lattice as revealed from Rietveld analysis for powder X-ray diffraction. The underdoped materials were observed to first undergo spin pairing transition in the temperature range well above T_c, and come across with superconducting transition at T_c. It was found that the spin gap temperature increases as the concentration of holes decreases, and vice versa for T_c. The results are in qualitatively good agreement with theoretical predictions from the mean-field RVB model [4].

2. EXPERIMENTS

The compounds of $R_{1+x}Ba_{2-x}Cu_3O_{7-\delta}$ were prepared by a conventional solid-state reaction. High-purity (>99.9%) reagent-grade $BaCO_3$, CuO, Nd_2O_3, or Eu_2O_3 in stoichiometric proportions was thoroughly mixed by grinding the oxides together in a mortar. The powders were repeatedly calcined in Al_2O_3 crucibles at 900°C in air for 24 h. The product was then isostatically pressed into disks with a diameter of about 1 cm in a steel die. The disks were then sintered 24 h in oxygen atmosphere at either 990°C or 1065°C. Subsequently they were annealed at 450°C in oxygen atmosphere for another 24 h. A Rigaku RU 200 12 kW X-ray generator with Cu K_α radiation (λ = 1.5418 Å) was used to perform powder X-ray diffraction (XRD) measurements with 2θ step scans taken for every 0.05° ranging from 20° to 120°. The crystalline structural information of the compounds was obtained through the Rietveld refinement method [16]. The resistivity measurements (RT) were carried out using a standard four-probe technique over a temperature range of 10 K to 300 K, where measuring leads are gold wires attached to the sample using indium contact.

3. RESULTS AND DISCUSSIONS

The samples of underdoped $Eu_{1+x}Ba_{2-x}Cu_3O_{7-\delta}$ sintered at 1065°C for $x \le 0.2$ are determined to be of pure phase through XRD analysis. Minor impurities are detected for the presence of unknown peaks at 2θ~28° in the XRD for $x \ge 0.3$ as shown in Fig. 1. Using Rietveld analysis, the compounds are determined to have orthorhombic structure of space group *Pmmm*, with the weight proportion reliability factors R_{wp} less than 4%. The results are listed in Table I. It was found that the lattice parameter ***a*** increases from 3.8434 Å to 3.8599 Å with the dopant concentration as shown in Fig. 2. Conversely, ***b*** and ***c*** decrease from 3.9005 Å and 11.713 Å to 3.8690 Å and 11.653 Å respectively. The volume of the unit cell was found to decrease from 175.599 $Å^3$ to 174.022 $Å^3$, as shown in Fig. 3. It implies that the bigger ions were replaced by the smaller ones in the dopant states. The ionic radius of Eu is 17% less than that of Ba and 60% greater than that of Cu. It is concluded that the excess Eu ions would predominantly occupy the lattice sites of Ba in the substituting scheme. This is in agreement with the observation that a divergent result would

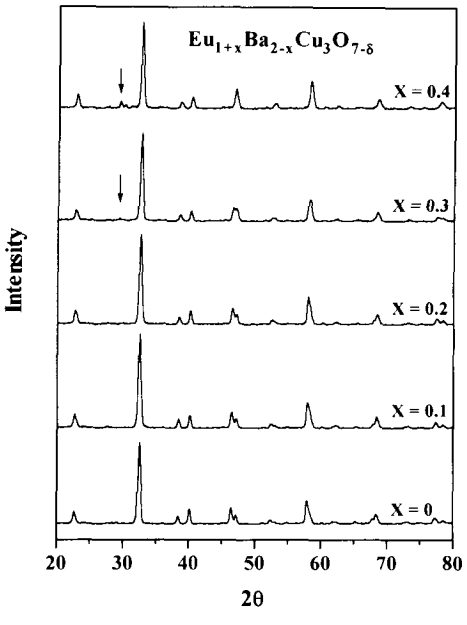

Fig. 1. The powder XRD patterns of the underdoped $Eu_{1+x}Ba_{2-x}Cu_3O_{7-\delta}$ sintered at 1065°C for $0 \le x \le 0.4$. The arrows are pointing at the unknown peaks at 2θ~28°.

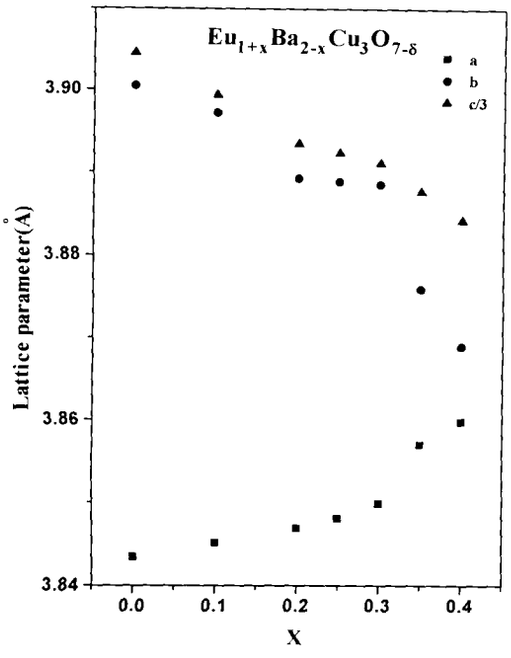

Fig. 2. The lattice parameters *a*, *b*, and *c* for the underdoped $Eu_{1+x}Ba_{2-x}Cu_3O_{7-\delta}$ sintered at 1065°C for $0 \leq x \leq 0.4$. The parameter *c* is represented by *c*/3 in the plot.

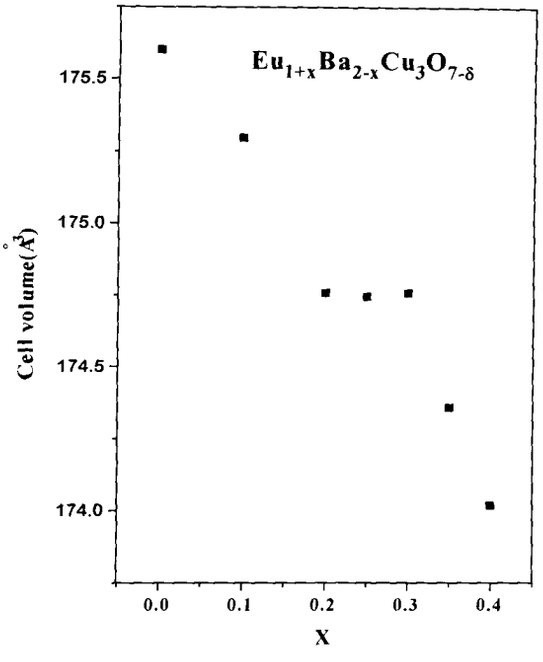

Fig. 3. The cell volume for the underdoped $Eu_{1+x}Ba_{2-x}Cu_3O_{7-\delta}$ sintered at 1065°C for $0 \leq x \leq 0.4$.

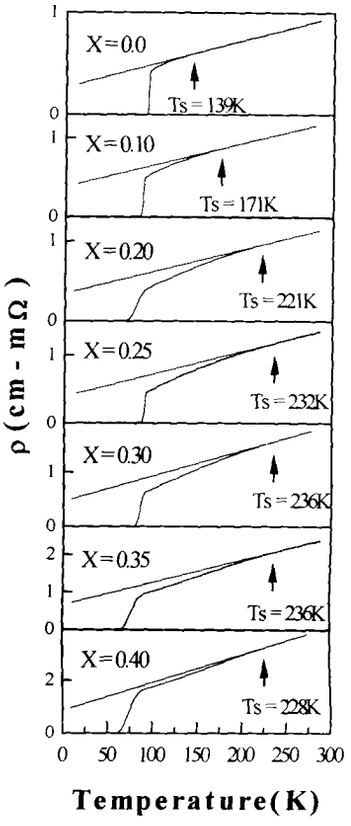

Fig. 4. The resistivity measurements of the underdoped $Eu_{1+x}Ba_{2-x}Cu_3O_{7-\delta}$ sintered at 1065°C for $0 \leq x \leq \leqq 0.4$.

occur if Cu sites were assumed to be occupied by the excess Eu ions during Rietveld analysis.

The electronic transport properties of $Eu_{1+x}Ba_{2-x}Cu_3O_{7-\delta}$ were investigated and the resistivity was observed to increase as the dopant concentration increases, except for $x = 0.2$ as shown in Fig. 4. Their superconducting transition temperature was found to decrease from 94 K, which is only slightly higher than previously reported: 90 K [17] for $x = 0$ to 84 K for $x = 0.4$. T_s of the compound is determined using the linear curve fitting scheme, adopted by François *et al.* [18], where a straight line, fitted for RT in the temperature range between 270 K and 260 K, is stretched out into the lower temperature region to examine the occurrence of the deviation of RT from linearity. And the T_s determined in this manner is subjected to a deviation of ±2 K, which is acceptable in this study. The correlations among T_s, T_c and the dopant concentrations are best depicted in Fig. 5, where T_s is observed to increase linearly from 139 K for $x = 0$, then start saturating at 232 K for $x = 0.25$ and peak at 236 K for $x = 0.3$, while a sudden rise of T_c at $x = 0.25$ is also observed in spite of its general

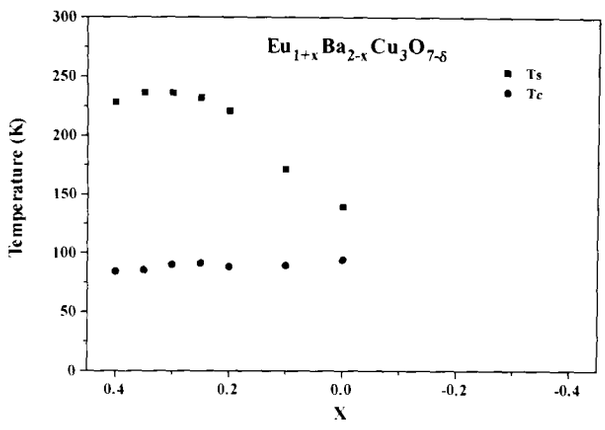

Fig. 5. T_s and T_c are plotted against the dopant concentration for the underdoped $Eu_{1+x}Ba_{2-x}Cu_3O_{7-\delta}$ sintered at 1065°C for $0 \leq x \leq 0.4$.

decreasing feature. These abrupt changes in T_c and T_s may be due to the complexity arising from the existence of the impurity in the samples for $x \geq 0.25$.

The powder XRD patterns of the underdoped $Nd_{1+x}Ba_{2-x}Cu_3O_{7-\delta}$ sintered at 990°C are plotted in Fig. 6. Samples are found to be of pure phase for $x \geq 0.2$. Minor unidentified phases were detected for $x \leq 0.2$ due to the presence of unknown peaks at $2\theta \sim 28°$ in their corresponding XRD patterns. Through Rietveld analysis the compounds are determined to have orthorhombic structure of space group *Pmmm* except for $x = 0.4$, which belongs to the tetragonal structure of space group *P4/mmm*. The factors R_{wp} are less than 3.5% as listed in Table II. The relation between the lattice parameters and the dopant concentration is shown in Fig. 7, where the lattice

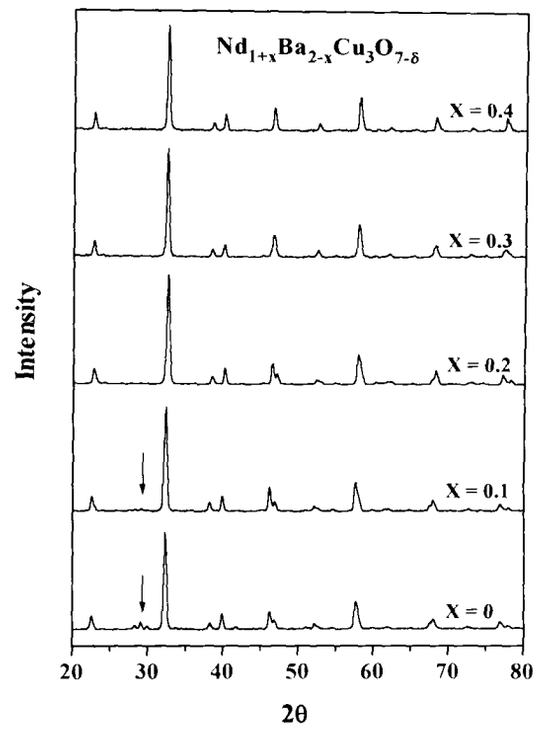

Fig. 6. The powder XRD patterns of the underdoped $Nd_{1+x}Ba_{2-x}Cu_3O_{7-\delta}$ sintered at 990°C for $0 \leq x \leq 0.4$.

parameter ***a*** increases from 3.8675 Å to 3.8871 Å, while ***b*** and ***c*** decrease from 3.9139 Å and 11.743 Å to 3.8871 Å and 11.675 Å respectively. And the cell volume, again, decreases from 177.768 $Å^3$ to 176.402 $Å^3$ as shown in Fig. 8. Thus, it is appropriate to assume that the excess Nd ions prefer the lattice sites of Ba in the substituting scheme since the ionic radius of Nd is 20% less than that of Ba and 56%

Table I. The Structural Parameters of $Eu_{1+x}Ba_{2-x}Cu_3O_{7-\delta}$ Sintered at 1065°C

x	a(Å)	b(Å)	c(Å)	V(Å^3)	R_p%	R_{wp}%	Space group
0	3.8434 (3)	3.9005 (5)	11.713 (2)	175.599	2.33	3.26	*Pmmm*
0.1	3.8451 (4)	3.8972 (6)	11.698 (1)	175.296	1.69	2.44	*Pmmm*
0.2	3.8469 (3)	3.8893 (4)	11.680 (1)	174.759	1.63	2.27	*Pmmm*
0.25	3.8481 (4)	3.8889 (6)	11.677 (2)	174.746	2.21	3.24	*Pmmm*
0.3	3.8499 (4)	3.8886 (5)	11.673 (2)	174.579	1.92	2.64	*Pmmm*
0.35	3.8571 (7)	3.8762 (1)	11.663 (3)	174.365	2.64	3.90	*Pmmm*
0.4	3.8599 (1)	3.8690 (1)	11.653 (2)	174.022	2.00	3.29	*Pmmm*

Table II. The Structural Parameters of $Nd_{1+x}Ba_{2-x}Cu_3O_{7-\delta}$ Sintered at 990°C

x	a(Å)	b(Å)	c(Å)	V(Å^3)	R_p%	R_{wp}%	Space group
0	3.8675 (3)	3.9139 (1)	11.743 (1)	177.768	2.34	3.47	*Pmmm*
0.1	3.8622 (2)	3.9126 (4)	11.749 (1)	177.554	1.94	2.71	*Pmmm*
0.2	3.8643 (3)	3.9137 (4)	11.735 (1)	177.247	1.89	2.73	*Pmmm*
0.3	3.8792 (3)	3.8935 (4)	11.707 (8)	176.822	1.67	2.45	*Pmmm*
0.4	3.8871 (2)	3.8871 (2)	11.675 (1)	176.402	1.88	2.87	*P4/mmm*

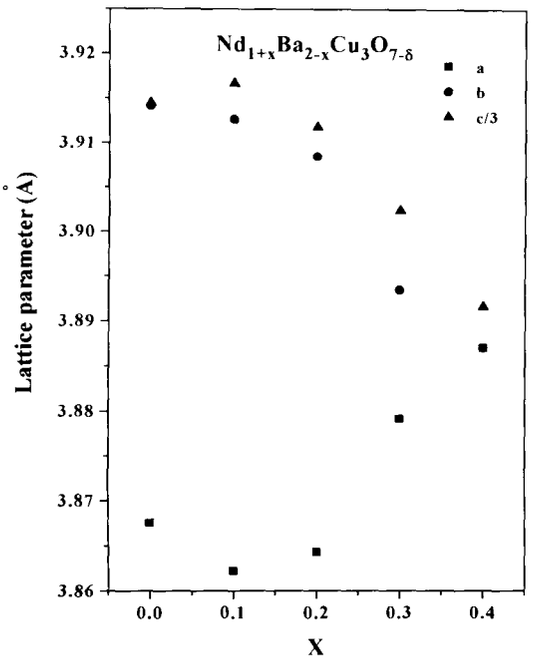

Fig. 7. The lattice parameters *a*, *b*, and *c* for the underdoped $Nd_{1+x}Ba_{2-x}Cu_3O_{7-\delta}$ sintered at 990°C for $0 \le x \le 0.4$. The parameter *c* is represented by *c*/3 in the plot.

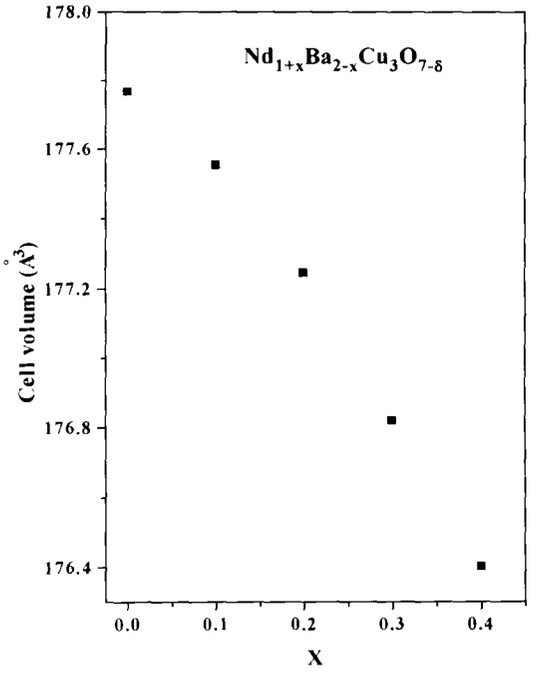

Fig. 8. The cell volume for the underdoped $Nd_{1+x}Ba_{2-x}Cu_3O_{7-\delta}$ sintered at 990°C for $0 \le x \le 0.4$.

greater than that of Cu. More evidence is provided with the observation that a divergent result would occur if Cu sites were assumed to be occupied by the excess Nd ions during Rietveld refinements.

The resistivity of $Nd_{1+x}Ba_{2-x}Cu_3O_{7-\delta}$ was observed to increase as the dopant concentration increased, as shown in Fig. 9, where T_c decreases from 96 K, comparable with the previous finding [19], to 25 K. T_s is observed to exhibit a remarkable linear dependence from 173 K to 218 K. The correlation among T_s, T_c, and the dopant concentrations is compared with the mean-field phase diagram of the RVB model as shown in Fig. 10. The deviation of T_c from the prediction for the optimal doping state is estimated to be 80 K, which is twice that of $Eu_{1+x}Ba_{2-x}Cu_3O_{7-\delta}$. However, the remarkable linearity of T_s as predicted from the RVB model was observed experimentally.

To summarize, the spin gap effect on the bulk system of $R_{1+x}Ba_{2-x}Cu_3O_{7-\delta}$, where R= Eu or Nd and $0 \le x \le 0.4$ was investigated. The underdoping states were achieved by alternatively substituting R^{3+} for Ba^{2+} ions in the system rather than adjusting the

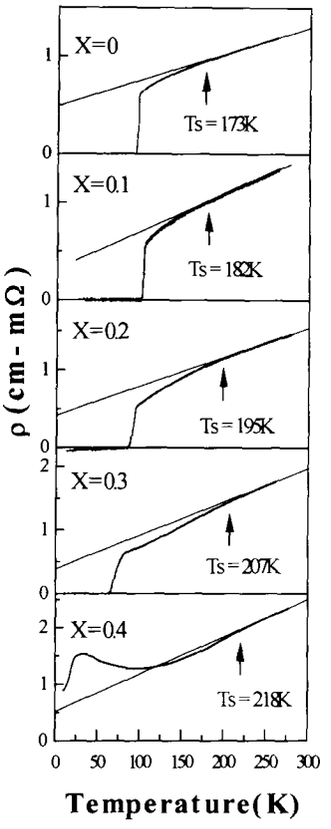

Fig. 9. The resistivity measurements of the underdoped $Nd_{1+x}Ba_{2-x}Cu_3O_{7-\delta}$ sintered at 990°C for $0 \le x \le 0.4$.

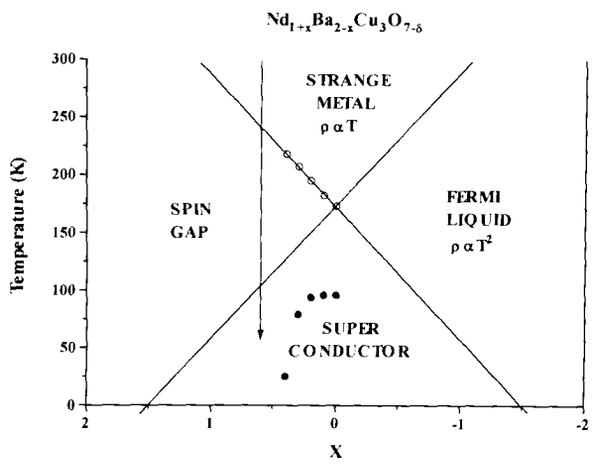

Fig. 10. T_s and T_c are plotted against the dopant concentration for the underdoped $Nd_{1+x}Ba_{2-x}Cu_3O_{7-\delta}$ sintered at 990°C for $0 \leq x \leq 0.4$. It is compared with the mean-field phase diagram based on the RVB model.

oxygen deficiency. The electronic transport properties of the bulk materials at various underdoping states were examined. The behavior of T_s and T_c is observed to be in support of the mean-field RVB model. However, there is a temperature difference of 40 K and 80 K, in contrast to zero as predicted, between T_s and T_c at the optimal doping state in each studied case respectively. In conventional BCS theory the opening of the superconducting gap and the transiting of the phase were to occur simultaneously. Recently, Wen and Lee [20] proposed, based on SU(2) mean-field calculations, that the charge and the spin of the carriers were to be separated into holons and spinons respectively. The spinons, which are paired to open the spin gap in the temperature range well above T_c, would condensate and become superconducting only if the coherence of the phases of the holons is reached below T_c. Thus, the normal-state property of high-T_c material is believed to be extremely closely related to the high-T_c mechanism. Great interests are centered on underdoping states of high-T_c materials for their exceptional normal-state properties that the energy gap is ready and it will become superconducting when the temperature is right.

ACKNOWLEDGMENTS

This study was supported by the National Science Council, R.O.C. Grant No. NSC86-2112-M-032-007.

REFERENCES

1. P. W. Anderson, *Science* **235**, 1196 (1987).
2. J. G. Bednorz and K. A. Muller, *Z. Phys. B* **64**, 189 (1986).
3. M. K. Wu, J. R. Ashburn, C. T. Torng, P. H. Hor, R. L. Meng, L. Gao, Z. J. Huang, Y. Q. Wang, and C. W. Chu, *Phys. Rev. Lett.* **58**, 908 (1987).
4. N. Nagaosa and P. A. Lee, *Phys. Rev. B* **45**, 966 (1992).
5. V. J. Emery and S. A. Kivelson, *Nature* **374**, 433 (1995).
6. W. W. Warren Jr., R. E. Walstedt, G. F. Brennert, R. J. Cava, R. Tycho, R. F. Bell, and G. Dabbagh, *Phys. Rev. Lett.* **62**, 1193 (1989).
7. M. Matsumura, Y. Sakamoto, T. Fushihara, Y. Itoh, and H. Yamagata, *J. Phys. Soc. Jpn.* **64**, 721 (1995).
8. H. Yasuoda, T. Imai, and T. Shimizu, in *Strong Correlation and Superconductivity*, H. Fukuyama, S. Maekawa, and A. P. Malozemoff, eds. (Springer, Berlin, 1989), p. 254.
9. J. Rossat-Mignod, L. P. Regnault, C. Vettier, P. Bourges, P. Burlet, J. Bossy, J. Y. Henry, and G. Lapertot, *Physica C* **185–189**, 86 (1991).
10. M. Tranquada, P. M. Gehring, and G. Shirane, *Phys. Rev. B* **46**, 5561 (1992).
11. H. Ding, T. Yokoya, J. C. Campuzano, T. Takahashi, M. Randeria, M. R. Norman, T. Mochiku, K. Kadowaki, and J. Giapintzakis, *Nature* **382**, 51 (1996).
12. A. G. Loeser, Z. X. Shen, D. S. Dessau, D. S. Marshall, C. H. Park, P. Fournier, and A. Kapitulnik, *Science* **273**, 325 (1996).
13. T. Ito, K. Takenaka, and S. Uchida, *Phys. Rev. Lett.* **70**, 3995 (1993).
14. K. Takenaka, K. Mizuhashi, H. Takagi, and S. Uchida, *Phys. Rev. B* **50**, 6534 (1994).
15. B. Bucher, P. Steiner, J. Karpinski, E. Kaldis, and P. Wachter, *Phys. Rev. Lett.* **70**, 20212 (1993).
16. *The Rietveld Method*, R. Y. Young, ed. (International Union of Crys., Oxford Univ. Press, 1993).
17. C. W. Chu, Z. J. Huang, R. L. Meng, L. Gao, and P. H. Hor, *Phys. Rev. B* **37**, 9730 (1988).
18. I. François, J. Genoe, and G. Borghs, *Phys. Rev. B* **54**, 3066 (1996).
19. H. Shked, B. W. Veal, J. Faber Jr., R. L. Hitterman, U. Balachandran, G. Tomlins, H. Shi, L. Morss, and A. P. Paulikas, *Phys. Rev. B* **41**, 4173 (1990).
20. X. G. Wen and P. A. Lee, *Phys. Rev. Lett.* **71**, 503 (1996).